Streptavidin-Enzyme Linked Aggregates for the One-Step Assembly and Purification of Enzyme Cascades

Hendrik Mallin*[a] and Thomas R. Ward*[a]

Abstract: Herein, we report on enzyme aggregates assembled around covalently cross-linked streptavidin tetramers. The streptavidin oligomeric matrix (Sav^{Matrix}) is produced using the SpyTag – SpyCatch technology and binds tightly to fusion proteins bearing a streptavidin-binding peptide (SBP). Fusing the SBPs to different enzymes leads to precipitation of the streptavidin-enzyme aggregates upon mixing the complementary components. This straightforward strategy can be applied to crude cell-free extract, allowing the one-step assembly and purification of catalytically active aggregates. Enzyme cascade assemblies can be produced upon adding different SBP-fused enzymes to the Sav^{Matrix}. The reaction rate for lactate dehydrogenase (LDH) is improved tenfold (compared to the soluble enzyme) upon precipitation with the Sav^{Matrix} from crude cell-free extracts. Additionally, the kinetic parameters are improved. A cascade combining a transaminase with LDH for the synthesis of enantiopure amines from prochiral ketones displays nearly threefold rate enhancement for the synthesis of (*R*)-α-methylbenzylamine compared to the free enzymes in solution.

Introduction

Enzymes have been used for several decades for the production of both bulk and high added-value compounds.[1] Thanks to significant progress in protein engineering and directed evolution, the so-called third wave of biocatalysts has begun to supplant established industrial processes.[2] Reactor design and immobilization strategies have also played a critical role in the recent success of industrial biotechnology.[3] Finally, the integration of complex pathways in production strains by metabolic engineering enables the production of both high-added value and bulk chemicals. This is achieved by engineering enzyme cascades.[4] The impact of biocatalysis on the production of industrial and pharmaceutically-relevant compounds are illustrated by the following selected examples: artemisinic acid (Sanofi-Aventis), 1,4-butane diol (Genomatica) and the Nylon-6 process (DSM).[5]

Efficient reaction pathways in nature often rely on the close proximity of the partner enzymes or on compartmentalization with sequential or cascade reactions. This prevents intermediate accumulation and side reactions as illustrated in glycolysis or the TCA-cycle.[6] High reactions rates are achieved thanks to the guided assembly- and scaffolding of the enzymes. Mimicking such enzyme assemblies and their application in systems biocatalysis is an active area of investigation.[7] For example, Dueber et al. designed a recombinant *E. coli* strain integrating an overexpressed mevalonate pathway by the use of specific protein-protein interaction domains on a specific protein scaffold.[8] The resulting reaction rates of the cascade were improved by 77 fold *in vivo*. Other elegant examples rely on designer cellulosomes or DNA scaffolds.[9] Such protein or DNA scaffolds allow to simply mix these components with the target enzymes to spontaneously afford the desired assembly. Insoluble aggregates are of special interest as they can be readily isolated by centrifugation to afford a purified solid displaying a desired activity. Insoluble cross-linked enzyme aggregates (CLEAs) are formed by mixing crude cell extracts with glutaraldehyde.[10] Despite their simplicity, these methods suffer from the unspecificity of the cross-linking step, which is best applied to (semi)-purified enzyme samples. Furthermore, structurally- or catalytically relevant lysine residues may react with glutaraldehyde thus leading to inactive CLEAs.[11] Alternatively, deactivation could result from the shortness of the glutaraldehyde spacer, limiting the access to the substrate to the active site of the immobilized enzymes or leading to (partial) denaturation of the enzyme.

In the approach presented herein, we set out to design an inert protein scaffold that would present highly specific binding moieties allowing to precipitate enzymes bearing a complementary binding motif. For this purpose, we selected the mature T7-tagged full-length streptavidin (Sav hereafter) as scaffolding protein. Thanks to its remarkable affinity for biotin and stability, Sav is used in many applications.[12] This versatile "molecular velcro" offers two key features: 1) Mature T7-tagged full-length Sav is highly soluble and can be expressed in high yield in *E. coli* with up to 8.3 $g \cdot L_{culture\ broth}^{-1}$.[13] This contrasts with core streptavidin which is produced as inclusion bodies. 2) In addition to its biotin-binding affinity, Sav binds streptavidin binding peptides (SBP hereafter) with high specificity and affinity. These short *N*- or *C*-fused peptides (e.g. Streptag, Nanotag, SBP-tag) are biocompatible and have found a broad range of application in biotechnology.[14] Sinclair *et al*. described the formation of 2D-protein lattices from core Sav with Streptagl-tagged proteins.[15] Although enzymes were used for this study, no information on the catalytic activity of the resulting 2D-network was provided. The resulting assemblies were small and poorly ordered arrays were achieved.[16] Herein, we report on our efforts to create enzyme aggregates relying on a streptavidin matrix amenable to the precipitation of enzymes from crude samples.

[a] Dr. Hendrik Mallin and Prof. Thomas R. Ward
Department of Chemistry
University of Basel
Mattenstrasse 24a, BPR 1096, CH-4058 Basel, Switzerland
thomas.ward@unibas.ch

Supporting information for this article is given via a link at the end of the document.

Results and Discussion

We hypothesized that cross-linking a highly soluble Sav may result in a (soluble) Sav matrix (Sav^{Matrix} hereafter) that could maintain its biotin binding sites available for subsequent anchoring and precipitation of SBP-tagged proteins. This may be achieved upon mixing crude cell free extract (CFE hereafter) containing the Sav^{Matrix} with CFE of SBP tagged enzymes (Scheme 1).

For the design of the oligomeric and functional Sav matrix from Sav tetramers, we selected the Spy-Tag/Spy-Catch domains from fibronectin-binding protein FbaB from *Streptococcus pyogenes*. This versatile system was adopted in view of its robust and rapid covalent isopeptide bond formation between the Catch- and the Tag domain in CFE.[17] This covalent bond formation was shown to work equally well in *in vitro* and *in vivo.* By placing the Spy-Tag or the Spy-Catch fragments either at the *C*- or the *N*-terminus of Sav, we anticipated that SBP-containing proteins may still bind the Sav^{Matrix}. Upon mixing both Sav^{Matrix} and crude SBP-tagged enzymes, a catalytically active and insoluble aggregate may result. Three challenges were identified in this context:

i) Can a soluble Sav^{Matrix} be produced relying on the SpyCatch-Tag domains?

ii) Can this matrix be cross-linked by SBP-tagged enzymes resulting in insoluble, enzyme aggregates?

iii) Can different SBP-tagged enzymes be simultaneously precipitated with the Sav^{Matrix} to achieve immobilized cascade reactions?

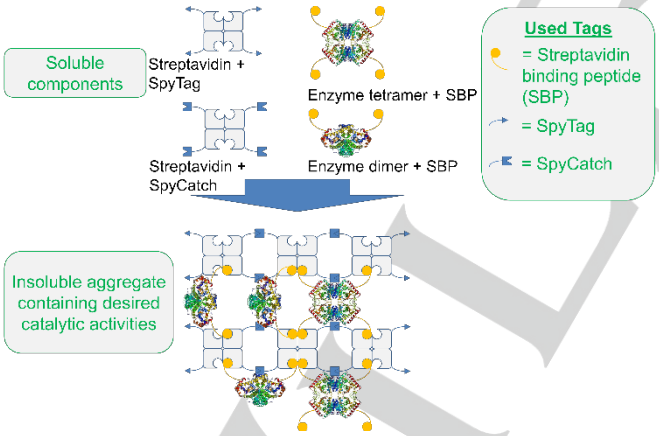

Scheme 1. Schematic representation of an artificial protein aggregate using a designed soluble oligomeric streptavidin matrix and SBP-tagged enzymes as building blocks. The multimeric enzymes act as cross-linker between the streptavidin matrix. The matrix is covalently assembled using the Spy-Tag-Catch protein interaction domains fused to streptavidin.

Design of a Streptavidin Spy-Tag/ Spy-Catch Matrix

For Sav^{Matrix} design, soluble oligotetrameric streptavidin assemblies were prepared using the Spy-Catch-Tag domains from fibronectin-binding protein FbaB from *Streptococcus pyogenes.*[17-18] This Spy-Tag-Catch system was selected in view of its robustness (against extreme pH, detergents etc.), fast covalent isopeptide bond formation and broad applicability. Furthermore, remarkable examples of enzyme-stabilization by cyclisation or attachment to *E. coli* nanofibers are reported using the Spy-Tag/Spy-Catch technology.[19]

The Sav^{Matrix} was produced *in vitro* by combining *E. coli* CFE of Sav fused to the Spy-Tag-domain (Sav^{SpyTag} hereafter) with Sav CFE fused to the Spy-Catch-domain (Sav^{SpyCatch} hereafter). Mixing both components leads to the spontaneous formation of a covalent isopeptide bond between the tag- and catch domain even in crude cell extracts. Thanks to the tetrameric nature of Sav, oligomeric structures should be formed (i.e. consisting of at least two tetramers). For the Spy-Catch domain, an optimized 84 amino acid long version (i.e. 32 amino acid shorter than wild-type) was selected for optimal expression yields.[18] The Tactin mutation (amino acids loop E44-S45-A46-V47 within Sav^{wildtype} mutated to E44V-S45T-A46-V47R) was introduced into the Sav to increase its affinity for the Streptag II.[20] First, the best protein termini (*N*- or *C*-) for fusion of the Spy-Tag or Spy-Catch domain to Sav were explored. The domains were fused to Sav using a ten amino acid linker (GGSIDGRGGS). The *N*-terminal Sav^{SpyTag} with the *N*-terminal Sav^{SpyCatch} gave the best yield of Sav^{Matrix} and were thus used for the rest of the study (See SI, Figure S1 and Table S3). Following this procedure, soluble oligotetramers of varying sizes (Figure S1, > 170 kDa) were formed thanks to the spontaneous isopeptide bond formation between the Spy-Tag and the Spy-Catch interaction domains.

Analytical size-exclusion chromatography of the Sav^{SpyTag} or Sav^{SpyCatch} single components (Table SI 5) revealed Sav^{SpyTag} and Sav^{SpyCatch} tetramers within the *E. coli* CFE (Table SI 5). Upon mixing both Sav components in equimolar ratio, very little residual Sav tetramers were detected by SDS-PAGE and size exclusion chromatography. This confirmed the versatility of the spontaneous covalent assembly even in the presence of cellular debris (Figure S1). Importantly, all Sav constructs, including the Sav^{Matrix}, bind biotin-4-fluorescein (B4F hereafter) on SDS-PAGE, highlighting the properly folded and accessible Sav binding pocket, despite the presence of chaotropic SDS. In view of the exquisite selectivity of the SBP-tags and the high concentration of soluble Sav in the CFE after expression, the crude Sav^{Matrix} containing-solutions was used for subsequent enzyme precipitation studies.

Enzyme Selection and Design

To investigate the ability of the Sav^{Matrix} to bind SBP-tagged proteins and form aggregates, six enzymes were selected (Scheme 2): A) A (*R*)-transaminase from *Neosartorya fischeri* ((*R*)-TA hereafter, dimeric) and a (*S*)-selective transaminase

from *Chromobacterium violaceum* ((*S*)-TA hereafter, dimeric), B) an alcohol dehydrogenase from *Lactobacillus kefir* (ADH hereafter, tetrameric), C) a lactate dehydrogenase from *Bacillus stearothermophilus* (LDH hereafter, dimeric according to SEC analysis), D) a phenylacetone monooxygenase from *Thermobifida fusca* (BVMO-Tf hereafter, monomeric) and E) a cyclohexanone monooxygenase from *Acinetobacter calcoaceticus* (BVMO-Ac hereafter, monomeric). These enzymes were tagged with two different streptavidin binding peptides: i) either the Streptag-II (SII- hereafter) or ii) the SBP-II tag. i) The Streptag-II is an eight amino acid peptide which binds with μM affinity to one Sav binding pocket and ii) The SBPII-tag, a 25 amino acid sequence, binds simultaneously to two adjacent Sav binding pockets with nM affinity. A limitation using genetically-encoded peptide tags is that the modification of the terminus could influence the enzyme's performance and expression. It is crucial to initially test the best termini or to rely on literature precedent. References using peptide tags to purify a specific enzyme may help in selecting the right termini. In the context of cascades, a reduction of the activity of the first enzyme could have a high negative impact on the final product yield.

All tested enzymes could be genetically tagged with the SII at their *N*-terminus. For LDH and (*S*)-TA additional variants were produced that included both SII and SBPII (*N*-terminal: Streptag-II and *C*-terminal: SBP-II, LDH-double and (*S*)-TA-double hereafter). This resulted in different binding behavior of the different enzyme variants depending on their quaternary structure (Table S4). A single SII-tagged enzyme monomer is expected to bind to only one Sav biotin binding pocket whereas the doubly tagged version can bind up to three pockets per monomer (SII- binds one and SBPII-tag binds two pockets).

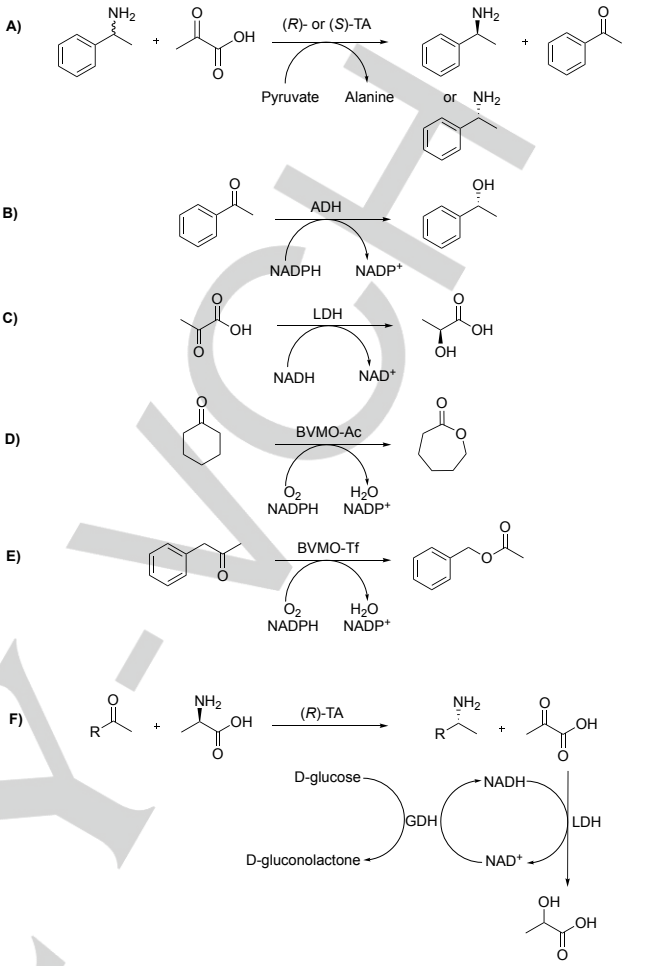

Scheme 2. Enzymatic reactions and corresponding cascade investigated in this study. A) Kinetic resolution of racemic amines with an (*R*)- or (*S*)- selective TA. The acetophenone product is readily detected 245 nm.[21] B) Acetophenone reduction to (*R*)-1-phenylethanol with an alcohol dehydrogenase. C) Pyruvate reduction L-lactate with a lactate dehydrogenase. D) Baeyer-Villiger oxidation of phenylacetone to benzyl acetate with BVMO-Tf. E) Baeyer-Villiger oxidation of cyclohexanone to ε-caprolactone with BVMO-Ac. For B) to E) monitoring of the reaction progress is achieved by spectrophotometry 340 nm reflecting the concentration of NAD(P)H. F) A three enzyme cascade for the synthesis of enantiopure amines from prochiral ketones. Both (*R*)-TA and LDH bear an SBP-tag while commercial glucose dehydrogenase were used.

Except for glucose dehydrogenase used for the regeneration of NAD^+ to NADH, all other enzymes were engineered to include Sav-binding peptides (Table S4). The recombinant overexpression was performed in *E. coli* BL21 (DE3). The resulting activities of the enzymes selected for further studies are collected in Table S4. The concentration of the overexpressed tagged-enzymes in the CFE was determined using a quantitative SDS-PAGE analysis for all samples.

Aggregates containing single enzymes

In an initial screen, each enzyme was incubated individually with the Sav^{Matrix}. Mixing was performed using equimolar amounts of enzyme and Sav free biotin binding sites (0.5 mM Sav monomer). The Sav^{Matrix} was mixed with the CFE containing the SII-enzyme. After incubation for three hours at 4 °C in the presence of Sav^{Matrix}, a turbid suspension was obtained for all enzymes except for the monomeric BVMOs (Figure S2, A and B examples given). Upon mixing with Sav^{Matrix}, the (*S*)-TA-double precipitated but the LDH-double remained in solution.

A solid pellet was obtained after centrifugation. To remove residual, unspecifically-bound proteins from the aggregates, the pellets were subjected to three consecutive washing steps using the corresponding enzyme buffers. The washing fractions were analyzed by SDS-PAGE and the protein content was determined (Figure S3): Nearly no residual protein was detected in the third fraction and only minimal amounts were present in the first two fractions. This suggests that two washing steps are sufficient to remove any unspecifically-bound enzyme. No detectable decrease in the pellet weight was observed during washing. This was determined by weighting the wet pellet (triplicates).

Table 1. Summary of the initial activities of the enzyme aggregates. The activity was determined at 30°C.

Entry	Enzyme variant	U g^{-1} dry aggregate [a, b]	Recovered activity % [c]	Precipitation Efficiency % [d]
1	LDH	167156 ± 2340	1086	31
2	ADH	5220 ± 489	111	74
3	(*R*)-TA	7986 ± 275	118	70
4	(*S*)-TA	1767 ± 29	44	6
5	(*S*)-TA-double	7068 ± 98	163	56
6	LDH purified	246188 ± 8546	452	68
7	(*R*)-TA purified	7390 ± 247	93	65

[a] Activity calculated for the whole protein aggregate amount (including enzyme and Sav^{matrix}). [b] Activity determined using 30 mM pyruvate (LDH), 10 mM acetophenone (ADH), 5 mM (*R*)-α-MBA ((*R*)-TA) or 5 mM (*S*)-α-MBA ((*S*)-TA). [c] Calculated by comparing the reduced activity from the supernatant after precipitation with the activity determined in the precipitate; [d] Calculated by comparing the activity of the supernatant after precipitation with the total activity prior to precipitation. Reaction conditions: 1 to 4 ml reaction volume (depending on activity), 5 to 50 µL of precipitate-enzyme suspension, 30°C (water temperate) using a VarianScan, buffers were preheated to 30°C, 2 to 5 min reaction time, Table S2 contains the corresponding enzyme buffers and pH.

The initial activity of the aggregates was determined using standard substrates (Table S2, Scheme 2). Initial activity tests using LDH aggregate resuspended by a short sonication step (10 s sonication, 5 cycles, 30% power) resulted in a twenty five-fold increased activity compared to the aggregate resuspended by pipetting. This effect could be observed for the other enzymes as well. However, it was less pronounced. As no detrimental effect was ever observed, this sonication step was systematically implemented prior to the activity-determination. We believe this results in an improved homogeneity of the solution and accessibility of the enzymes. The highest activities (Table 1, entry 1 and 3) were obtained with the LDH and (*R*)-TA aggregates. Good activities were also obtained for the ADH and the (*S*)-TA-double (Table 1, entry 2 and 5). The activity of the (*S*)-TA was significantly lower (Table 1, entry 4) highlighting the better performance of the (*S*)-TA-double. The initial screen of the enzyme variants highlighted the generality of the method as all tested multimeric enzymes could be precipitated resulting in high volumetric enzymatic activity and with full recovery of the activity (calculated from units absent from the supernatant after precipitation *versus* units in the aggregate). Freeze-drying of the enzyme suspensions (resuspended in the corresponding enzyme buffer after washing of the aggregate) offers a straightforward means to store the aggregates: No loss of activity was observed for the freeze-dried LDH. All aggregates could be stored in 50 % glycerol at -20 °C. The glycerol is easily removed by centrifugation and washing. Short-term storage up to two weeks at 4 °C is possible for all aggregates.

For the rest of the study, the LDH and the (*R*)-TA were selected as benchmark enzymes for the formation of aggregates. Both were isolated from thermophile organisms and displayed good precipitation properties. They were obtained in sufficient amounts by recombinant expression in *E. coli*. Accordingly, the LDH and (*R*)-TA were recombinantly expressed and purified by Streptag affinity chromatography. Upon mixing purified LDH with the Sav^{Matrix}, the LDH aggregates displayed 47 % higher volumetric activity and higher efficiency (twice as high compared to CFE, Table 1, entry 1 and 6). The efficiency was calculated by comparing the reduced activity of the supernatant after precipitation to the initial activity of the enzyme prior to precipitation: 100 % refers to no activity in the supernantant after precipitation. Aggregates from CFE containing (*R*)-TA displayed comparable activities to those resulting from purified (*R*)-TA (Table 1, entry 3 and 7).

Next, free- and aggregated (*R*)-TAs were tested for the asymmetric amine synthesis from prochiral ketones (Scheme 2, F). To shift the equilibrium to the amine, soluble glucose dehydrogenase (GDH) was combined with LDH. Commercial rabbit muscle LDH was used as we anticipated that the SII-tagged LDH may displace the (*R*)-TA bound to the Sav^{Matrix}. Both acetophenone and 2-hexanone were selected as benchmark substrates. After 48 h, comparable conversions and enantioselectivities were obtained for the free- and (*R*)-TA aggregates. This highlights that the (*R*)-TA performance is not negatively affected upon formation of the aggregate.

For the LDH aggregate, a tenfold improvement in activity was observed using LDH CFE. A less pronounced improvement (4.5 fold) was obtained for the purified LDH. Next, the kinetic parameters for the free LDH and the LDH aggregates were determined for both pyruvate and NADH (Table 2).

Table 2. Kinetic parameters of LDH and LDH aggregates for pyruvate and

NADH.[a]

Entry	LDH sample	Substrate[b]	K_m [mM]	k_{cat} [s^{-1}]	k_{cat}/K_m ($s^{-1}\cdot\mu M^{-1}$)	K_i [mM]
1	Free purified	Pyruvate	14.6 ± 4.6	59	4,046	119 ± 5
2	Aggregate	Pyruvate	5.7 ± 3.4	98	17,164	94 ± 5
3	Free purified	NADH	0.13 ± 0.03	74	572,718	-
4	Aggregate	NADH	0.055 ± 0.007	135	2,450,078	-

[a] Values were determined by monitoring the decrease in absorbance of NADH at 340 nm and 30°C. [b] For the saturation kinetics analysis, both pyruvate and NADH were added to the LDH, and a single substrate concentration was varied at a time. Apparent kinetics are given.

Reaction conditions: 4 ml reaction volume, 30°C (water temperate) using a VarianScan, MES-Buffer (100 mM, pH 6.5) was preheated to 30°C, 5 min reaction time, reaction was initiated by addition of 50 µL of purified free LDH or precipitate-LDH suspension (13 µg ml^{-1}) followed by immediate mixing.

Regarding pyruvate (Table 2, entry 1 and 2), the aggregate outperformed the free LDH: the K_m decreased by 2.6 fold, the k_{cat} improved by 1.7 fold; accordingly the k_{cat} / K_m increased by 4.2 fold. For NADH (Table 2, entry 3 and 4), the same trend was observed: The K_m decreased by 2.4 fold, the k_{cat} improved by 1.8 fold and the k_{cat} / K_m by 4.3 fold. The improvement for the k_{cat} / K_m values were congruent with the observed improved performance of the aggregate obtained with the purified LDH (Table 1, entry 6, 4.5 fold). Although the observed difference between free and aggregated LDH for the K_m value for pyruvate was within the experimental error, the same trend in K_m decrease was observed using NADH as benchmark substrate. The LDH displays substrate inhibition at high pyruvate concentrations[22]. NADH binds first to LDH, followed by pyruvate to form the catalytically active complex. After reduction, the LDH-NAD^+-lactate complex is obtained, leading to the release of lactate upon turnover. At high concentrations of pyruvate, the inactive LDH-NAD^+-pyruvate binary complex is formed leading to LDH inhibition. The substrate inhibition is slightly affected by the aggregate, which displays a decreased K_i compared to the free enzyme.

The minimal loading of the Sav^{Matrix} was determined using the purified LDH as Strep-tagged enzyme. The amount of matrix (0.5 mM FBS) was kept constant and the enzyme loading was varied incrementally from 0.16 to 1.34 equivalents vs. FBS sites of the Sav^{Matrix} (See Figure S4). At low LDH concentration, very little activity was detected; at 0.65 equivalents, the activity increased to 61 % of the maximal activity which was obtained at 1.34 equivalents (100 %). Using a Boltzman fit, we determined that 0.56 ± 0.15 equivalents LDH vs. Sav FBS lead to 50 % activity. We conclude that minimum loading amount of the Sav^{Matrix} required to induce precipitation of enzyme is equal to 0.5 eq. of enzyme vs FBS.

Influence of the Oligomeric State of the Tagged Enzyme on Agglomeration

While the tested monomeric enzymes bearing a single Streptag moiety do not led to the formation of an insoluble aggregate, precipitation can be achieved with multimeric enzymes upon mixing with Sav^{Matrix}. Insoluble aggregates are obtained for oligomeric enzymes presenting 2-6 biotin binding modules (SBP = two modules, SII = one module). Unfortunately, the monomeric BVMOs containing two biotin binding modules could not be isolated. Next, we verified that the designed Sav^{Matrix} afforded the best activity upon mixing with multimeric enzymes. For this purpose, (*R*)-TA was selected as model enzyme and was mixed with different Sav variants (0.5 mM Sav FBS): i) full-length $Sav^{wildtype}$ ii) full-length Sav containing the StrepTactin mutation (hereafter Sav^{Tactin}) iii) Sav^{Spytag}, iv) $Sav^{SpyCatch}$ and v) Sav^{Matrix} (Figure 1).

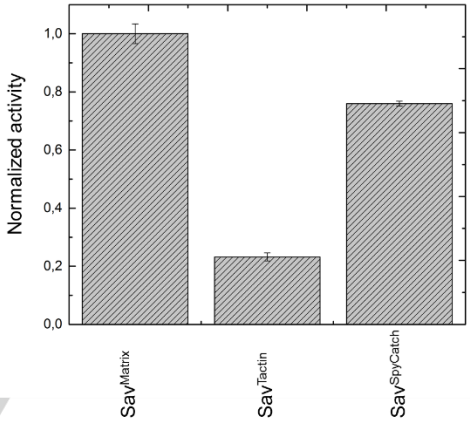

Figure 1. Relative activities of (*R*)-transaminase aggregates using different Sav-variants. Sav^{Tactin}: Sav-wild type containing the SII-tag binding domain. Both the Sav^{SpyTag} and the $Sav^{wildtype}$ do not form aggregates upon addition of (*R*)-TA and are thus not displayed. A normalized activity of 1 refers to 7990 U $g^{-1}_{dry\ aggregate}$. Reaction conditions: 3 ml reaction volume, 30°C (water temperate) using a VarianScan, sodium phosphate buffer (50 mM, pH 7.5) was preheated to 30°C, 5 mM (*R*)-α-methylbenzylamine and 5 mM pyruvate, 5 min reaction time, reaction was initiated by addition of 10 µL precipitate-(*R*)-TA suspension followed by immediate mixing, monitored at 245 nm (a UV cuvette was used).

Inspection of Figure 1 reveals that, except for both Sav^{SpyTag} and $Sav^{wildtype}$, the three other Sav-variants yield an active aggregate upon mixing with *(R)*-TA. The Sav^{Matrix} displayed the highest activity which was normalized to 1 for comparison. The Sav^{Tactin} (tetramer) displayed only 20 % activity, suggesting that the oligomeric state of Sav plays a critical role in the aggregate's activity. Accordingly, the $Sav^{SpyCatch}$ displayed only 75 % activity compared to the aggregate resulting from Sav^{Matrix}. We speculate that the size of the Catch-protein ($Sav^{SpyCatch}$ M_W = 100 kDa) favours precipitation upon addition of the tagged *(R)*-TA.

Cascades Resulting from Co-precipitation of Two Enzymes with Sav^{Matrix}

Next, three enzymes were selected to engineer a cascade for the synthesis of enantiopure amines from prochiral ketones. For this purpose, the (*R*)-TA, GDH and LDH were selected as benchmark cascade (Scheme 2, F). The commercial, non-tagged GDH was added as free enzyme to the suspension. A two-enzyme aggregate was assembled by co-precipitating (*R*)-TA and LDH with Sav^{Matrix} (LDH/(*R*)-TA^{co} hereafter). Both enzymes were mixed in equimolar amounts prior to mixing with equimolar amounts of FBS present in Sav^{Matrix}. After 3 h, the turbid suspension was centrifuged and the pellet was washed. The initial activities of both enzymes were determined individually using the respective standard substrates (Scheme 2, A and C). Gratifyingly, both enzymes were active in the aggregate. For all cascade experiments, the same starting activities of the (*R*)-TA and LDH were used. The LDH/(*R*)-TA^{co} aggregate was compared to the soluble enzymes or to the separately-aggregated (*R*)-TA and LDH (LDH/(*R*)-TA^{sep} hereafter). Remarkably, in the presence of the LDH/(*R*)-TA^{co} aggregate, the yields of (*R*)-α-methylbenzylamine and (*R)*-2-aminohexane were improved by 2.9 fold and 1.4 fold after 48 h respectively compared to the free enzymes and the LDH/(*R*)-TA^{sep} (Figure 2). Very similar yields were obtained for the free enzymes compared to the LDH/(*R*)-TA^{sep}. This suggests a synergistic effect upon co-aggregating both enzymes within the Sav^{Matrix}. In all experiments, the enantioselectivity of the amine exceeded (*R*)-99 %.

Figure 2. Amine concentration determined after 48 hours resulting from a

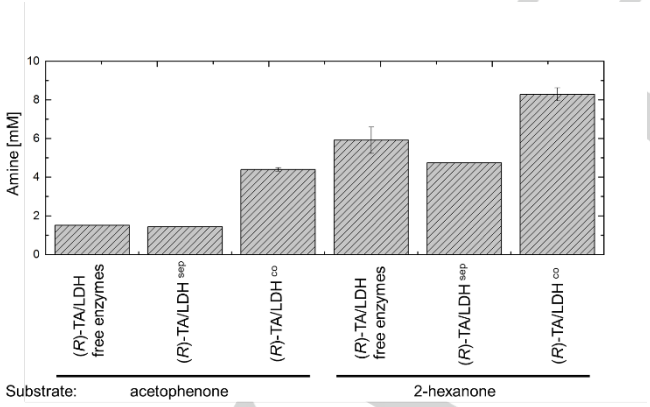

cascade that combines (*R*)-TA and LDH in the presence of prochiral ketones. The free enzymes were compared to separately- (sep) and (co) aggregated (*R*)-TA and LDH. Commercial glucose dehydrogenase was added as soluble enzyme in all experiments. Reaction conditions: 0.2 ml reaction volume, 30°C, sodium phosphate buffer (50 mM, pH 7.5, 0.1 mM pyridoxalphoshat), ketone substrate (25 mM), DMSO (10 %), D-alanine (125 mM), D-glucose (150 mM), 15 U ml^{-1} GDH-105 (Codexis, Redwood City), 3.5 U ml^{-1} LDH (activity against pyruvate) and 0.8 U ml^{-1} (*R*)-TA (activity against (*R*)-α-methylbenzylamine), the activities were normalized in each approach to allow for direct comparison. Analyses were performed by HPLC (conversion) and GC (enantioselectivity), see SI.

Conclusions

In summary, a novel matrix based on streptavidin for the formation of enzyme aggregates was designed. In the presence of enzymes bearing a Sav-binding peptide tag, catalytically active aggregates can be precipitated from *E. coli* crude cell extracts. Full recovery of the enzymatic activity was demonstrated for four enzymes from different classes. Several tag combinations were evaluated and the best was identified for each enzyme. The activity of the LDH aggregate was improved by nearly fivefold (up to 246188 U $g^{-1}_{dry\ aggregate}$). (*R*)-α-methylbenzylamine and (*R*)-2-aminohexane were produced from a cascade which included LDH, (*R*)-TA and soluble GDH (for NADH regeneration). The yield was improved by nearly threefold for co-aggregates combining LDH and (*R*)-TA. To the best of our knowledge this study is the first example of an oligo-tetrameric Sav^{Matrix}, which is produced recombinantly in high yield. This method resembles a carrier-free approach, where a natural protein is used as crosslinking agent displaying specific affinity with the target proteins. The target protein can be obtained in higher purity in a one-step batch approach which may enable straightforward up-scaling. As all building blocks are genetically encoded, the system may be amenable to *in vivo* enzyme assembly. The method could thus be an attractive addition to the toolbox of synthetic biology to create artificial, scaffolded cell factories.

Experimental Section

For experimental details see supporting data.

Acknowledgements

The authors thank the NCCR molecular systems engineering, the ERC (the DrEAM) and the SNF (grant 200020 162348) for financial support. We thank Noah Naef for help with the initial experiments.

Keywords: Protein Precipitation • Protein-Crosslink • Biocatalysis • Protein Design • Enzyme Cascades

Reference list

[1] a) K. Buchholz, V. Kasche, U. T. Bornscheuer, *Biocatalysts and Enzyme Technology*, *2nd ed*., Wiley-VCH, Weinheim, **2012**; b) N. J. Turner, E. O'Reilly, *Nat. Chem. Biol.* **2013**, *9*, 285-288; c) A. Liese, K. Seelbach, C. Wandrey, *Industrial Biotransformations*, Wiley-VCH, Weinheim, **2000**; d) H. Sun, H. Zhang, E. L. Ang, H. Zhao, *Bioorgan. Med. Chem.* **2017**; e) O. May, H.

Gröger, W. Drauz, *Enzymes in Organic Synthesis*, Wiley-VCH, Weinheim, **2012**.

[2] a) U. T. Bornscheuer, G. W. Huisman, R. J. Kazlauskas, S. Lutz, J. C. Moore, K. Robins, *Nature* **2012**, *485*, 185-194; b) C. K. Savile, J. M. Janey, E. C. Mundorff, J. C. Moore, S. Tam, W. R. Jarvis, J. C. Colbeck, A. Krebber, F. J. Fleitz, J. Brands, P. N. Devine, G. W. Huisman, G. J. Hughes, *Science* **2010**, *329*, 305-309; c) A. A. Desai, *Angew. Chem. Int. Ed.* **2011**, *50*, 1974-1976; d) M. T. Reetz, *J. Am. Chem. Soc.* **2013**, *135*, 12480-12496; e) Y. Miao, M. Rahimi, E. M. Geertsema, G. J. Poelarends, *Curr. Opin. Chem. Biol.* **2015**, *25*, 115-123; f) C. K. Prier, F. H. Arnold, *J. Am. Chem. Soc.* **2015**, *137*, 13992-14006; g) H. Renata, Z. J. Wang, F. H. Arnold, *Angew. Chem. Int. Ed.* **2015**, *54*, 3351-3367.

[3] a) U. Hanefeld, L. Cao, E. Magner, *Chem. Soc. Rev.* **2013**, *42*, 6211-6212; b) A. Liese, L. Hilterhaus, *Chem. Soc. Rev.* **2013**, *42*, 6223-6235; c) L. Zhao, Q. Liu, S. Yan, Z. Chen, J. Chen, X. Li, *J. Biotechnol.* **2013**, *168*, 46-54; d) R. A. Sheldon, S. van Pelt, *Chem. Soc. Rev.* **2013**, *42*, 6223-6235; e) B. M. Nestl, B. A. Nebel, B. Hauer, *Curr. Opin. Chem. Biol.* **2011**, *15*, 187-193; f) H. Mallin, J. Muschiol, E. Byström, U. Bornscheuer, *Chemcatchem* **2013**, *5*, 3529-3532; g) K. B. Otte, B. Hauer, *Curr. Opin. Biotechn.* **2015**, *35*, 16-22.

[4] a) A. S. Bommarius, *Annu. Rev. Chem. Biomol. Eng.* **2015**, *6*, 319-345; b) L. J. Hepworth, S. P. France, S. Hussain, P. Both, N. J. Turner, S. L. Flitsch, *Acs Catal.* **2017**, *7*, 2920-2925; c) M. Hönig, P. Sondermann, N. J. Turner, E. M. Carreira, *Angew. Chem. Int. Ed.* ***2017***, *56*, *8942-8973;* d) J. H. Schrittwieser, S. Velikogne, M. Hall, W. Kroutil, *Chem. Rev.* **2017**, *118*, 270–348; e) V. Köhler, Y. M. Wilson, M. Dürrenberger, D. Ghislieri, E. Churakova, T. Quinto, L. Knörr, D. Häussinger, F. Hollmann, N. J. Turner, T. R. Ward, *Nat. Chem.* **2013**, *5*, 93-99.

[5] a) D. K. Ro, E. M. Paradise, M. Ouellet, K. J. Fisher, K. L. Newman, J. M. Ndungu, K. A. Ho, R. A. Eachus, T. S. Ham, J. Kirby, M. C. Chang, S. T. Withers, Y. Shiba, R. Sarpong, J. D. Keasling, *Nature* **2006**, *440*, 940-943; b) H. Yim, R. Haselbeck, W. Niu, C. Pujol-Baxley, A. Burgard, J. Boldt, J. Khandurina, J. D. Trawick, R. E. Osterhout, R. Stephen, J. Estadilla, S. Teisan, H. B. Schreyer, S. Andrae, T. H. Yang, S. Y. Lee, M. J. Burk, S. Van Dien, *Nat. Chem. Biol.* **2011**, *7*, 445-452; c) S. C. H. J. Turk, W. P. Kloosterman, D. K. Ninaber, K. P. A. M. Kolen, J. Knutova, E. Suir, M. Schürmann, P. C. Raemakers-Franken, M. Müller, S. M. A. de Wildeman, L. M. Raamsdonk, R. van der Pol, L. Wu, M. F. Temudo, R. A. M. van der Hoeven, M. Akeroyd, R. E. van der Stoel, H. J. Noorman, R. A. L. Bovenberg, A. C. Trefzer, *ACS Synth. Biol.* **2016**, *5*, 65-73.

[6] a) W. C. Plaxton, *Annu. Rev. Plant. Physiol. Plant. Mol. Biol.* **1996**, *47*, 185-214; b) R. K. Thauer, *Eur. J. Biochem.* **1988**, *176*, 497-508.

[7] a) H. Hirakawa, T. Haga, T. Nagamune, *Top. Catal.* **2012**, *55*, 1124-1137; b) I. Wheeldon, S. D. Minteer, S. Banta, S. C. Barton, P. Atanassov, M. Sigman, *Nat. Chem.* **2016**, *8*, 299-309; c) C. Schmidt-Dannert, F. Lopez-Gallego, *Microb. Biotechnol.* **2016**, *9*, 601-609.

[8] J. E. Dueber, G. C. Wu, G. R. Malmirchegini, T. S. Moon, C. J. Petzold, A. V. Ullal, K. L. J. Prather, J. D. Keasling, *Nat. Biotech.* **2009**, *27*, 753-759.

[9] a) C. M. Fontes, H. J. Gilbert, *Annu. Rev. Biochem.* **2010**, *79*, 655-681; b) L. Xia, K. Van Nguyen, Y. Holade, H. Han, K. Dooley, P. Atanassov, S. Banta, S. D. Minteer, *ACS Energy Lett.* **2017**, *2*, 1435-1438.

[10] R. A. Sheldon, W. R. K. Schoevaart, L. M. van Langen, *Biocatal. Biotransfor.***2005,** 23, 141-147.

[11] a) L. Cao, L. Langen, R. A. Sheldon, *Curr. Opin. Biotechnol.* **2003**, *14*, 387-394; b) S. Velasco-Lozano, F. López-Gallego, J. Mateos-Díaz, E. Favela-Torres, *Biocatalysis* **2016***, 1*, 166-177; c) J. Cui, S. Jia, L. Liang, Y. Zhao, Y. Feng, *Sci. Rep.* **2015**, *5*, 14203; d) S. S. Nadar, R. G. Pawar, V. K. Rathod, *Int. J. Biol. Macromol.* **2017**, *101*, 931-957; e) J. D. Cui, S. R. Jia, *Crit. Rev. Biotechnol.* **2015**, *35*, 15-28.

[12] C. M. Dundas, D. Demonte, S. Park, *Appl. Microbiol. Biotechnol.* **2013**, *97*, 9343-9353.

[13] a) T. Sano, C. R. Cantor, *PNAS* **1990**, *87*, 142-146; b) M. Jeschek, M. O. Bahls, V. Schneider, P. Marliere, T. R. Ward, S. Panke, *Metab. Eng.* **2017**, *40*, 33-40.

[14] a) T. G. M. Schmidt, A. Skerra, *J. Chromatogr.* **1994**, *676*, 337-345; b) A. Skerra, T. G. M. Schmidt, *Methods Enzymol.* **2000***, 326,* 271-304; c) A. D. Keefe, D. S. Wilson, B. Seelig, J. W. Szostak, *Protein. Expres. Purif.* **2001**, *23*, 440-446.

[15] a) J. C. Sinclair, K. M. Davies, C. Venien-Bryan, M. E. M. Noble, *Nat. Nano.* **2011**, *6*, 558-562; b) P. Ringler, G. E. Schulz, *Science* **2003**, *302*, 106-109.

[16] J. C. Sinclair, *Curr. Opin. Chem. Biol.* **2013**, 6.

[17] B. Zakeri, J. O. Fierer, E. Celik, E. C. Chittock, U. Schwarz-Linek, V. T. Moy, M. Howarth, *PNAS* **2012,** *109***,** 690-697.

[18] L. Li, J. O. Fierer, T. A. Rapoport, M. Howarth, *J. Mol. Biol.* **2014**, *426*, 309-317.

[19] a) C. Schöne, J. O. Fierer, S. P. Bennett, M. Howarth, *Angew. Chem. Int. Ed.* **2014**, 53, 6101–6104; b) C. Schöne, S. P. Bennett, M. Howarth, *Sci. Rep.* **2016**, *6*, 21151; c) Z. Botyanszki, P. K. R. Tay, P. Q. Nguyen, M. G. Nussbaumer, N. S. Joshi, *Biotechnol. Bioeng.* **2015**, *112*, 2016-2024.

[20] S. Voss, A. Skerra, *Prot. Engin.* **1997**, *10*, 975-982.

[21] S. Schätzle, M. Höhne, E. Redestad, K. Robins, U. T. Bornscheuer, *Anal. Chem.* **2009**, *81*, 8244-8248.

[22] H. Gutfreund, R. Cantwell, C. H. McMurray, R. S. Criddle, G. Hathaway, *Biochemical Journal* **1968**, *106*, 683-687.

Entry for the Table of Contents (Please choose one layout)

Layout 1:

FULL PAPER

Graphical Abstract Insoluble protein assemblies that combine streptavidin aggregates and streptagged enzymes display increased activity for systems biocatalysis.

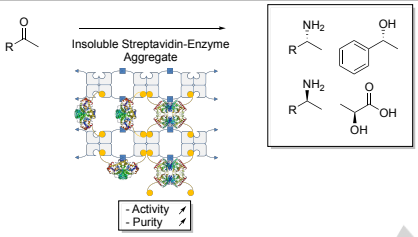

Hendrik Mallin and Thomas R. Ward

Page No. – Page No.

Streptavidin-Enzyme Linked Aggregates for the One-Step Assembly and Purification of Enzyme Cascades